

Tracking Performance under Time Delay and Asynchronicity in Distributed Camera Systems

Klementyna Szwaykowska, Fumin Zhang, Wayne Wolf

Abstract—Distributed camera systems are typically used to simultaneously track multiple targets. Communication between cameras enables the ability to monitor targets in a complex environment where occlusion happens. Asynchronicity and time delay are among the most important factors that affect tracking error. We provide a feedback law controlling the pan and tilt of each camera to track the centroid of a cluster of point targets in the field of view. Assuming that the estimates for target motion are available only infrequently and asynchronously when occlusion happens, we compute a worst-case lower bound on the frequency for exchanging estimates between cameras. Our results may help camera system designers to determine the response time and tracking ability for distributed camera systems.

I. INTRODUCTION

Recent advancements in technology have dramatically reduced the cost of manufacturing and installing distributed camera systems. Research in image processing and computer vision has enabled using cameras to track moving targets with high accuracy in real time. Distributed camera systems have the advantage of cooperatively tracking targets even when occlusion happens in the field of view of some of the cameras in the network. Cameras with occlusion may request estimates of the blocked targets from other cameras monitoring the targets from different viewing angles. Communication delays and asynchronicity exist in most such distributed systems [1]. Controller design under time-delay has been a long lasting focus in the control literature c.f. [2]–[5]. The problem of asynchronicity has gained much recent interest due to the research thrusts in cooperative control and sensor networks [6]–[8].

There have been ongoing efforts to generalize Lyapunov stability theory to systems with hybrid nature [9]–[13]. In this paper, we develop methods based on input to state stability (ISS) for discrete-time systems [14]–[17] and apply them to a simplified perspective dynamic model [18]–[20] of the distributed camera systems to establish relationship between tracking error, delay, and asynchronicity. By explicitly determining an ISS Lyapunov function for the camera tracking system, one can estimate the size of a neighborhood to which the state will converge. This gives a measure of the system performance for different possible values of communication/computation delays and different control gains. Such a metric is highly desirable in applications involving

control/scheduler co-design; if a certain level of tracking performance is required, the state estimation/computation of the control law can be scheduled so that the control interval never exceeds a deadline, which we choose together with control gain and inter-measurement interval in such a way that the performance requirements are met.

In section II, we briefly review the perspective dynamics that model the motion of a point target in the image plane of a camera. We then introduce tracking controllers for a single camera to track one or a cluster of point targets in section III. In section IV, we consider the effect of time delay and asynchronicity on the tracking performance for two cameras tracking multiple targets. Simulation results will be presented in section V.

II. THE PERSPECTIVE DYNAMICAL SYSTEM

We consider cameras with controllable pan and tilt. We first introduce a model that describes the motion of a point target in the image plane of a camera.

Consider a single camera which observes targets moving in the space \mathcal{R}^3 . We may establish the camera coordinate frame using three orthogonal unit vectors \mathbf{i} , \mathbf{j} , \mathbf{k} to define the three axes. The origin is located at the lens of the camera, and \mathbf{i} and \mathbf{j} span a plane that is parallel to the camera’s image plane. Hence \mathbf{k} is perpendicular to the image plane. Rotation around \mathbf{i} is the tilt motion and rotation around \mathbf{j} is the pan motion. We also define an inertial, or “lab”, frame whose origin coincides with that of the camera frame, and whose axes are initially aligned with the camera frame’s axes. When the pan and tilt motion are performed, the body, or “camera”, coordinate frame rotates with the camera. The orientation of the camera in the inertial frame can be described by a matrix $g \in SO(3)$ (that is, $gg^T = I$).

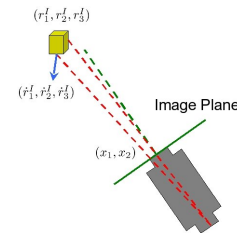


Fig. 1. Schematic of the perspective system

Let \mathbf{r}_I represent a point in \mathcal{R}^3 (see fig. 1). The position of the point in the camera’s coordinate frame is $\mathbf{r} = g^{-1}\mathbf{r}_I$. Multiplying both sides by g and taking time derivatives, we obtain $\dot{\mathbf{r}} = g(\Omega \times \mathbf{r} + \dot{\mathbf{r}})$, where $\Omega = \omega\mathbf{i} + \nu\mathbf{j} + 0\mathbf{k}$ is the

Klementyna Szwaykowska, Fumin Zhang, and Wayne Wolf are with School of Electrical and Computer Engineering, Georgia Institute of Technology. Email: klimka,fumin,wolf@ece.gatech.edu.

This research is supported by ONR grant N00014-08-1-1007 and NSF ECCS-0841195.

angular velocity of the camera, and u and v stand for the pan and tilt controls, respectively. If we define a velocity vector $\mathbf{b} = g^{-1}\dot{\mathbf{r}}_I$, we can write $\dot{\mathbf{r}} = -\Omega \times \mathbf{r} + \mathbf{b}$.

The vectors \mathbf{r} and \mathbf{b} may be decomposed as: $\mathbf{r} = r_1\mathbf{i} + r_2\mathbf{j} + r_3\mathbf{k}$ and $\mathbf{b} = b_1\mathbf{i} + b_2\mathbf{j} + b_3\mathbf{k}$. Consider the projection of \mathbf{r} on the image plane of the camera; the projected position can be described by $\mathbf{x} = x_1\mathbf{i} + x_2\mathbf{j}$, defined as follows:

$$x_1 = \frac{r_1}{r_3} \quad \text{and} \quad x_2 = \frac{r_2}{r_3} \quad (1)$$

We now derive the first-order perspective dynamics of the system. First, $\dot{\mathbf{r}} = -\Omega \times \mathbf{r} + \mathbf{b}$ implies that:

$$\begin{aligned} \dot{r}_1 &= b_1 - r_3v \\ \dot{r}_2 &= b_2 + r_3u \\ \dot{r}_3 &= b_3 - r_2u + r_1v. \end{aligned} \quad (2)$$

Let us define $B_i = b_i/r_3$ for $i = 1, 2, 3$. Taking the time derivatives of x_1 and x_2 , we have:

$$\dot{x}_1 = -\frac{r_1\dot{r}_3}{r_3^2} + \frac{\dot{r}_1}{r_3} = x_1x_2u - (x_1^2 + 1)v + B_1 - B_3x_1 \quad (3)$$

$$\dot{x}_2 = -\frac{r_2\dot{r}_3}{r_3^2} + \frac{\dot{r}_2}{r_3} = (x_2^2 + 1)u - x_1x_2v + B_2 - B_3x_2. \quad (4)$$

Note that x_1 , x_2 , B_1 , and B_2 may be estimated from measurements taken by the camera, since they represent the position and velocity of the point in the image plane, but B_3 cannot be estimated by any direct method.

In the target tracking problem, we want to control the value of x_1 and x_2 so that the target is always in the field of view. If the camera is far away from the target, it is reasonable to assume that B_3 is negligible. We can confine ourselves to the study of the following subsystem:

$$\begin{aligned} \dot{x}_1 &= x_1x_2u - (x_1^2 + 1)v + B_1 \\ \dot{x}_2 &= (x_2^2 + 1)u - x_1x_2v + B_2. \end{aligned} \quad (5)$$

In the following sections, we design controllers for the simplified perspective dynamics (5).

III. CONTROLLER DESIGN FOR SINGLE CAMERA

In this section, we study the problem of controlling a single camera to track multiple targets in continuous time. The control objective is to keep the centroid of the targets at the center of the camera's field of view (FOV). In the special case of single target tracking, the target is kept at the center of the FOV.

A. Tracking multiple targets with single camera

Suppose there are N targets. Their positions are given by \mathbf{x}_i , $i = 1, \dots, N$. The centroid is given by $\mathbf{x}_c = \frac{1}{N} \sum_{i=1}^N \mathbf{x}_i$; the motion of the centroid is given by:

$$\dot{\mathbf{x}}_c = \begin{bmatrix} \dot{x}_{c1} \\ \dot{x}_{c2} \end{bmatrix} = \begin{bmatrix} \frac{1}{N} \sum_i x_{i1}x_{i2}u - \frac{1}{N} \sum_i (x_{i1}^2 + 1)v + \frac{1}{N} \sum_i B_{i1} \\ \frac{1}{N} \sum_i (x_{i2}^2 + 1)u - \frac{1}{N} \sum_i x_{i1}x_{i2}v + \frac{1}{N} \sum_i B_{i2} \end{bmatrix} \quad (6)$$

where all sums are taken over $i = 1$ to N .

We now define the matrix

$$G_c = \frac{1}{N} \begin{bmatrix} \sum_{i=1}^N x_{i1}x_{i2} & \sum_{i=1}^N (x_{i1}^2 + 1) \\ \sum_{i=1}^N (x_{i2}^2 + 1) & \sum_{i=1}^N x_{i1}x_{i2} \end{bmatrix} \quad (7)$$

Using induction over i , one can verify that $\det(G_c) > 0$. Therefore, a linearizing control can be obtained by taking:

$$\begin{bmatrix} u \\ v \end{bmatrix} = G_c^{-1} \left(A \begin{bmatrix} x_{c1} \\ x_{c2} \end{bmatrix} - \frac{1}{N} \begin{bmatrix} \sum_{i=1}^N B_{i1} \\ \sum_{i=1}^N B_{i2} \end{bmatrix} \right) \quad (8)$$

where $A \in \mathbb{R}^2$ is an arbitrary Hurwitz matrix. In the idealized case that all the states are known exactly, the equilibrium state (which corresponds to the centroid being at the center of the FOV) is globally asymptotically stable.

IV. DISTRIBUTED CAMERAS AND DISCRETE CONTROLLERS

Occlusion happens when one or more targets are blocked by obstacles in the FOV of one camera. In this case, the camera may request updates of the blocked targets' positions from other nearby cameras. This direct communication is possible using cameras like those developed in [1]. The estimates so obtained, however, suffer time-delay and asynchronicity. We investigate how these factors affect the tracking error.

A typical pan and tilt camera has embedded computers that compute the control actions. Therefore, control commands are sent at discrete instants. We discretize the perspective dynamical system (5) under the assumption that the control for pan and tilt happens accurately at time instants t_k where $k = 0, 1, 2, \dots$, and $T = t_{k+1} - t_k$ is constant for all k . Let $G_{c,k} = G_c(t_k)$ and define

$$F_k = \begin{bmatrix} \sum_{i=1}^N B_{i,1}(t_k) \\ \sum_{i=1}^N B_{i,2}(t_k) \end{bmatrix}, \quad \mathbf{u}_k = \begin{bmatrix} u(t_k) \\ v(t_k) \end{bmatrix} \quad (9)$$

Then the discrete perspective dynamics for one camera are given by:

$$\mathbf{x}_c(t_{k+1}) = \mathbf{x}_c(t_k) + G_{c,k}\mathbf{u}_kT + F_{c,k}T \quad (10)$$

Consider the following setup. Camera $C1$ is tracking a set of N targets, some of which may be occluded; the goal is to maintain the centroid of the targets as close as possible to the center of the camera's FOV. The linearizing pan/tilt control \mathbf{u} (eq. (8)) for the camera is calculated with an interval of T seconds. Simultaneously with the release of each control command, the camera accepts a measurement of the image-plane position \mathbf{x} and velocity F of the target. Camera $C1$ communicates with other cameras in order to obtain measurements of position and velocity of the occluded obstacles. In order to reduce networking traffic, we assume that the communication between cameras happens infrequently, so that not all estimates made by these other cameras will be sent to $C1$. For example, if a camera has estimates available every 10ms, it may choose to send the estimates every 50ms. Therefore, at $C1$, estimates for occluded targets will be available less frequently than estimates for targets which have clear line of sight; we will

assume that the updates are available with period mT , where m is a positive integer, $m > 1$. In practical situations, both m and T may vary; we assume here that both are constant and known, and represent the worst-case delay.

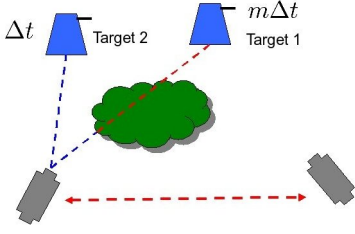


Fig. 2. Two-target tracking system with one occluded target

We analyze the simple case $N = 2$, with one target (say, target 1) occluded (see fig. 2). On the interval $[t_k, t_{k+m})$, then, measurements of \mathbf{x} and F for the unblocked target (target 2) are updated m times and those for the occluded target (target 1) are updated only once. This causes asynchronicity in the discretized system described by (10).

Note that due to computational and communication delays in the system, our control effort calculations at time t_j must rely on estimates of $\mathbf{x}_c(t_j)$ based on measurements made at some previous time, t_k , $k < j$. A simple estimator can be constructed to obtain the estimates (here denoted by hatted values) recursively as follows:

$$\begin{aligned} \mathbf{u}_j &= \hat{G}_{c,j}^{-1}(A\hat{\mathbf{x}}_c(t_j) - \hat{F}_{c,j}) \\ \hat{\mathbf{x}}_c(t_{j+1}) &= \mathbf{x}_c(t_j) + G_{c,j}\mathbf{u}_jT + F_{c,j}T \\ \hat{F}_{c,j+1} &= \hat{F}_{c,j} \end{aligned} \quad (11)$$

where $\mathbf{x}_c(t_k)$ and $F_{c,k}$ are the measured values of the target's position and velocity, respectively, and are assumed to be known exactly. If at time t_j a measurement of the state is not available, the $\hat{\mathbf{x}}_c(t_j)$ and $\hat{F}_{c,j}$ are taken as the exact values, so that $\mathbf{x}_c(t_j) = \hat{\mathbf{x}}_c(t_j)$ and $F_{c,j} = \hat{F}_{c,j}$ in the above equations.

We write $\hat{\mathbf{x}}_c(t_k)$ as $\hat{\mathbf{x}}_c(t_k) = \mathbf{x}_c(t_k) + \xi_k$, and $\hat{F}_{c,k} = F_{c,k} + \xi_k^F$, where ξ_k and ξ_k^F are the position estimation error and velocity estimation error, respectively. These errors usually grow with the length of the inter-measurement time mT . In this paper, we assume that for each target i , the position estimation error $\|\xi_{i,k}\|$ is bounded by $L(\Delta t)^q$, while $\|\xi_{i,k}^F\|$ is bounded by $L(\Delta t)^{q-1}$. Here $L \in \mathbb{R}^+$ and $q \in \mathbb{Z}^+$ are known constants, and Δt is the time since the last available measurement.

We pick A in (11) to be a diagonal matrix, $A = -K_k I$, where I is the 2×2 identity matrix, and K_k is a positive scalar which may be interpreted as an adjustable control gain. Minimizing $\|\hat{\mathbf{x}}_c(t_{k+1})\|$ with respect to K_k in eq. (11), we derive the optimal gain: $K_k = \frac{1}{T}$. In fact, neglecting estimation errors, this control gain would bring \mathbf{x}_c to $\mathbf{x}_c = 0$ in a single discrete-time step. However, since T is by assumption small, a control gain of $\frac{1}{T}$ may be physically impossible to implement. We therefore set $K_k = \frac{1}{\alpha T}$, where $\alpha > 1$, so that the control $\mathbf{u}_k = -K_k I \hat{\mathbf{x}}_c(t_k)$ will be less likely to exceed actuator limits.

We will now show that the tracking system described by (11), with A defined as above, is discrete-time input to state stable (ISS) (see [14] for definition); that is, the state \mathbf{x}_c converges to a small neighborhood of the center of $C1$'s FOV.

Lemma 4.1: Consider a single-target camera tracking system with dynamics described by eq. (10), with $N = 2$, inter-control input interval T , and inter-measurement intervals mT for target 1 and T for target 2. Matrix A and bounds on $\|\xi\|$ and $\|\xi^F\|$ are defined as above. Then the system is discrete-time input to state stable (ISS) and admits a quadratic Lyapunov function.

Proof: For $\|\xi\| \leq LT^q$, we assume that error due to imperfect knowledge of the state $\mathbf{x}_c(t_k)$ in calculating matrix \hat{G} may be absorbed into the estimation error of $\mathbf{x}_c(t_{k+1})$. Then (11) can be rewritten as a set of perturbed equations:

$$\begin{aligned} \mathbf{x}_c(t_{k+1}) &= (I + AT)\mathbf{x}_c(t_k) + \tilde{\mathbf{u}}_k \\ \tilde{\mathbf{u}}_k &= AT\xi_k + \xi_k^F T \end{aligned} \quad (12)$$

For any finite fixed T , this can be interpreted as a discrete-time plant with open-loop dynamics described by $\mathbf{x}_c(t_{k+1}) = (I + AT)\mathbf{x}_c(t_k)$, and a bounded stochastic input $\tilde{\mathbf{u}} = AT\xi_k + \xi_k^F T$.

With A defined as $A = \frac{1}{\alpha T}I$, $I + AT$ is a Schur matrix. Therefore, similar to Example 3.4 in [14], we can always find a quadratic discrete Lyapunov function for (12). Since our system admits an ISS Lyapunov function, it is necessarily ISS according to Lemma (3.5) in [14]. ■

The size h of the neighborhood to which V will converge depends on the magnitudes of estimation errors ξ and ξ^F . To find the value of h , we need the following two simple lemmas:

Lemma 4.2: Given a quadratic polynomial

$$p(x) = -ax^2 + bx + c$$

with $a, b, c \in \mathbb{R}^+$, $a \neq 0$, and a non-zero affine function

$$q(x) = dx + f$$

with $d, f \in \mathbb{R}^+$, there exists some $C > 0$ such that

$$(p + q)(x) < 0 \text{ for all } x > C$$

Proof: Let

$$C = \frac{(b + d) + \sqrt{(b + d)^2 + 4a(c + f)}}{2a} > 0$$

Then, $(p + q)(C) = 0$, and $\frac{d}{dx}(p + q) = (-2ax + (b + d))$ is strictly negative for all $x \geq C$. Therefore for $x > C$, $(p + q)(x) < 0$. ■

Lemma 4.3: Given an inequality $r(x) \leq s(x)$ for all $x > 0$, with

$$s(x) = ax^2 + bx + c$$

where $a, b, c \in \mathbb{R}^+$, $a \neq 0$, and $s(x = \phi) = \Phi$ for some $\phi > 0$, it follows that $r(x) \leq \Phi$ for all $0 < x \leq \phi$.

Proof: For all $x > 0$, $\frac{d}{dx}s(x) = 2ax + b > 0$. Therefore, $s(x)$ is a strictly increasing function of x for all $x > 0$, and it follows that $(x) \leq s(x) \leq \Phi$ for all $0 < x \leq \phi$. ■

We now turn to our tracking system. We explicitly define a Lyapunov function as follows:

$$V_k = \frac{1}{2} \mathbf{x}_c(t_k)^T \mathbf{x}_c(t_k) \quad (13)$$

We will analyze the behavior of this function over a time interval $(t_k, t_{k+m}]$, where we assume that measurements of the state of target 1 are available at times t_k and t_{k+m} , while measurements for target 2 are available at $t_k, t_{k+1}, \dots, t_{k+m}$. Note that $V_{k+m} - V_k$ can be written as:

$$V_{k+m} - V_k = V_{k+m} + \sum_{j=k+1}^{k+m-1} (-V_j + V_j) - V_k \quad (14)$$

Thus, to guarantee $V_{k+m} - V_k < 0$, it is sufficient to have $V_{j+1} - V_j < 0$ for all $j \in \{k, k+1, \dots, k+m-1\}$.

Lemma 4.4: Suppose we have a system defined by (10) and (8), with discrete ISS Lyapunov function given by (13). Then $V_{j+1} - V_j < 0$, $\forall j \in \{k, k+1, \dots, k+m-1\}$ whenever $\|x_c(t_j)\| > h_1$, where

$$h_1 = \frac{\alpha^2 L T^q \left(2 - \frac{1}{\alpha} - \frac{1}{\alpha^2} + \sqrt{4 + \frac{7}{\alpha^2} - \frac{2}{\alpha^3}} \right)}{2(2\alpha - 1)} \quad (15)$$

Proof: Since no new measurements for target 1 are available over (t_{k+1}, t_{k+m-1}) , the error in the state estimate of target 1 is assumed to be 0. Therefore, at these times, the only error contribution in estimates of \mathbf{x}_c is error in the state estimates for target 2: $\xi_k = \frac{1}{2} \xi_{2,k}$ and $\xi_k^F = \frac{1}{2} \xi_{2,k}^F$, where $\|\xi_2\| \leq L T^q$ and $\|\xi_2\| \leq L T^{q-1}$. We therefore write $V_{j+1} - V_j$ ($j \in \{k, k+1, \dots, k+m-1\}$) as:

$$V_{j+1} - V_j = V_{j+1} - \hat{V}_{j+1} + \hat{V}_{j+1} - V_j \quad (16)$$

and analyze $V_{j+1} - \hat{V}_{j+1}$ and $\hat{V}_{j+1} - V_j$ separately.

First, we consider $\hat{V}_{j+1} - V_j$. Note that for any i, j we can write:

$$\begin{aligned} V_j - V_i &= \frac{1}{2} \mathbf{x}_c(t_j)' \mathbf{x}_c(t_j) - \frac{1}{2} \mathbf{x}_c(t_i)' \mathbf{x}_c(t_i) \\ &= \mathbf{x}_c(t_i)' (\Delta \mathbf{x}_c) + \frac{1}{2} \Delta \mathbf{x}_c' \Delta \mathbf{x}_c \end{aligned} \quad (17)$$

where $\Delta \mathbf{x}_c = \mathbf{x}_c(t_j) - \mathbf{x}_c(t_i)$. Therefore we can write:

$$\hat{V}_{j+1} - V_j = \mathbf{x}_c(t_j)' \left(\frac{\hat{\mathbf{x}}_c(t_j)}{\alpha} + \xi_j^F T \right) + \frac{1}{2} \left\| \frac{\hat{\mathbf{x}}_c(t_j)}{\alpha} + \xi_j^F T \right\|^2$$

Applying bounds on ξ_k and ξ_k^F , we can define an upper bound on $\hat{V}_{j+1} - V_j$ as follows:

$$\begin{aligned} \hat{V}_{j+1} - V_j &\leq -\frac{1}{2} \left(\frac{2}{\alpha} - \frac{1}{\alpha^2} \right) \|x_c(t_j)\|^2 \\ &\quad + \frac{1}{2} \left(1 - \frac{1}{\alpha^2} \right) L T^q \|x_c(t_j)\| + \frac{1}{8} \left(1 + \frac{1}{\alpha} \right)^2 L^2 T^{2q} \end{aligned} \quad (18)$$

Similarly, $V_{j+1} - \hat{V}_{j+1}$ can be written as:

$$V_{j+1} - \hat{V}_{j+1} = (\mathbf{x}_c(t_{j+1}) + \xi_{j+1})' \xi_{j+1} + \frac{1}{2} \|\xi_{j+1}\|^2 \quad (19)$$

Which is bounded as:

$$V_{j+1} - \hat{V}_{j+1} \leq \frac{1}{2} \left(1 - \frac{1}{\alpha} \right) L T^q \|x_c(t_j)\| + \frac{1}{8} \left(1 + \frac{4}{\alpha} \right) L^2 T^{2q} \quad (20)$$

Applying Lemma 4.2 to (18) and (20), we see that $V_{j+1} - V_j < 0$ whenever $\|\mathbf{x}_c(t_j)\| > h_1$, where h_1 is given by (15). ■

Lemma 4.5: Suppose we have a system defined by (10) and (8), with discrete ISS Lyapunov function given by (13). Then

$$\max\{V_{k+1}, \dots, V_{k+m-1}\} \leq \max\{V_k, \frac{1}{2} h_1^2\}$$

where h_1 is defined as in (15).

Proof: First suppose that $x_c(t_k) > h_1$, corresponding to $V_k > \frac{1}{2} h_1^2$. By Lemma 4.4, this means that $V_{k+1} - V_k < 0$, so that $V_{k+1} < V_k$. By induction, $V_{j+1} < V_j < V_k$ holds for each $j \in \{k+1, \dots, k+m-1\}$ so long as $x_c(t_j) > h_1$.

Now suppose that for some j , $\|x_c(t_j)\| \leq h_1$. Then, adding equations (18) and (20) for time t_j , we get:

$$\begin{aligned} V_{j+1} - V_j &\leq -\frac{1}{2} \left(\frac{2}{\alpha} - \frac{1}{\alpha^2} \right) \|x_c(t_j)\|^2 \\ &\quad + \frac{1}{2} \left(2 - \frac{1}{\alpha} - \frac{1}{\alpha^2} \right) L T^q \|x_c(t_j)\| \\ &\quad + \frac{1}{8} \left(2 + \frac{6}{\alpha} + \frac{1}{\alpha^2} \right) L^2 T^{2q} \end{aligned} \quad (21)$$

Adding $V_j = \frac{1}{2} \|x_c(t_j)\|^2$ to both sides of the inequality, we see that:

$$\begin{aligned} V_{j+1} &\leq \frac{1}{2} \left(1 - \frac{1}{\alpha} \right)^2 \|x_c(t_j)\|^2 \\ &\quad + \frac{1}{2} \left(2 - \frac{1}{\alpha} - \frac{1}{\alpha^2} \right) L T^q \|x_c(t_j)\| \\ &\quad + \frac{1}{8} \left(2 + \frac{6}{\alpha} + \frac{1}{\alpha^2} \right) L^2 T^{2q} \\ &= \tilde{a} \|x_c(t_j)\|^2 + \tilde{b} \|x_c(t_j)\| + \tilde{c} \end{aligned} \quad (22)$$

where $\tilde{a}, \tilde{b}, \tilde{c}$ are strictly greater than 0 and $\tilde{a} h_1^2 + \tilde{b} h_1 + \tilde{c} = \frac{1}{2} h_1^2$. By Lemma 4.3, therefore, $V_{j+1} < \frac{1}{2} h_1^2$ for all $\|x_c(t_j)\| < h_1$.

We have shown that for all initial values V_k ,

$$\max\{V_{k+1}, \dots, V_{k+m}\} \leq \max\{V_k, \frac{1}{2} h_1^2\} \quad \blacksquare$$

Lemma 4.6: Suppose we have a system defined by (10) and (8), with discrete ISS Lyapunov function given by (13). Then there exists an $h_2 > h_1$ such that $V_{k+m} - V_{k+m-1} < 0$ for all $\|x_c(t_{k+m-1})\| > h_2$.

Proof: At time t_{k+m} , estimates of the states of both targets are available, so that the error in position is given by $\xi_{c,k+m} = \frac{1}{2} (\xi_{1,k+m} + \xi_{2,k+m})$, where $\xi_{1,k+m} \in \mathcal{X}$

with $\Delta t = mT$ and $\xi_{2,k+m} \in \mathcal{X}$ with $\Delta t = T$. The error in velocity is given by $\xi_{c,k+m}^F = \frac{1}{2}(\xi_{1,k+m}^F + \xi_{2,k+m}^F)$, where $\xi_{1,k+m}^F \in \mathcal{XF}$ with $\Delta t = mT$ and $\xi_{2,k+m}^F \in \mathcal{XF}$ with $\Delta t = T$. Thus, we can say that $\xi_{c,k+m} \in \{\phi : \|\phi\| \leq \frac{1}{2}(1+m^q)LT^q\}$ and $\xi_{c,k+m}^F \in \{\psi : \|\psi\| \leq \frac{1}{2}(1+m^{q-1})LT^{q-1}\}$.

We write $V_{k+m} - V_{k+m-1}$ as:

$$\begin{aligned} V_{k+m} - V_{k+m-1} \\ = V_{k+m} - \hat{V}_{k+m} + \hat{V}_{k+m} - V_{k+m-1} \end{aligned} \quad (23)$$

and analyze $V_{k+m} - \hat{V}_{k+m}$ and $\hat{V}_{k+m} - V_{k+m-1}$ separately.

It can be shown that:

$$\begin{aligned} \hat{V}_{k+m} - V_{k+m-1} &\leq -\frac{1}{2}\left(\frac{2}{\alpha} - \frac{1}{\alpha^2}\right) \|x_c(t_{k+m-1})\|^2 \\ &+ \frac{1}{2}\left(1 - \frac{1}{\alpha^2}\right)LT^q \|x_c(t_{k+m-1})\| + \frac{1}{8}\left(1 + \frac{1}{\alpha}\right)^2 L^2T^{2q} \end{aligned} \quad (24)$$

Then, we can find a bound on $V_{k+m} - \hat{V}_{k+m}$ as:

$$\begin{aligned} V_{k+m} - \hat{V}_{k+m} &\leq \frac{1}{2}\left(1 - \frac{1}{\alpha}\right) (1+m^q)LT^q \|x_c(t_{k+m-1})\| \\ &+ \frac{1}{8}\left(\frac{4}{\alpha}(1+m^q) + (1+m^q)^2\right) L^2T^{2q} \end{aligned} \quad (25)$$

Adding together equations (24) and (25) and applying Lemma 4.2, we see that $V_{k+m} - V_{k+m-1} < 0$ whenever $\|\mathbf{x}_c(t_j)\| > h_2$, where h_2 is given by:

$$h_2 = \frac{\alpha^2LT^q(2 - \frac{1}{\alpha} - \frac{1}{\alpha^2} + (1 - \frac{1}{\alpha})m^q + \sqrt{H})}{2(2\alpha - 1)} \quad (26)$$

where

$$H = 4 + \frac{7}{\alpha^2} - \frac{2}{\alpha^3} + \left(4 - \frac{6}{\alpha} + \frac{6}{\alpha^2} - \frac{2}{\alpha^3}\right)m^q + m^{2q} \quad (27)$$

Note that $h_2 > h_1$. \blacksquare

We are now ready to show that, as $t \rightarrow \infty$, \mathbf{x}_c stays within an invariant neighborhood of the center of the camera's FOV:

Theorem 4.1: Suppose we have a system defined by (10) and (8), with discrete ISS Lyapunov function given by (13). The position of target 1 is measured with interval mT , and that of target 2, with interval T . Then as $t_k \rightarrow \infty$, $\|\mathbf{x}_c\|$ is bounded above by h_2 , which is defined as in (26).

Proof: Consider a function W_k defined as $W_{k+m} = \max_{i \in \{k, k+m\}} V_i$. By Lemma 4.5, we know that

$$\max\{V_{k+1}, \dots, V_{k+m-1}\} \leq \max\{V_k, \frac{1}{2}h_1^2\}$$

where $h_1 < h_2$.

Suppose that $V_{k+m-1} > \frac{1}{2}h_2^2 > \frac{1}{2}h_1^2$. By Lemma 4.5, it follows that $V_{k+m-1} < V_k$. In this case, by Lemma 4.6, $V_{k+m} - V_{k+m-1} < 0$, so that $V_{k+m} < V_{k+m-1} < V_k$, and we have established that

$$\max\{V_{k+1}, \dots, V_{k+m-1}\} = V_k \leq \max\{V_k, \frac{1}{2}h_2^2\}$$

Now suppose that $V_{k+m-1} \leq \frac{1}{2}h_2^2$. Adding equations (24) and (25) for time t_{k+m-1} , we get:

$$\begin{aligned} V_{k+m} - V_{k+m-1} &\leq -\frac{1}{2}\left(\frac{2}{\alpha} - \frac{1}{\alpha^2}\right) \|x_c(t_{k+m-1})\|^2 \\ &+ \frac{1}{2}\left(1 - \frac{1}{\alpha^2} + \left(1 - \frac{1}{\alpha}\right)(1+m^q)\right)LT^q \|x_c(t_{k+m-1})\| \\ &+ \frac{1}{8}\left(\left(1 + \frac{1}{\alpha}\right)^2 + \frac{4}{\alpha}(1+m^q) + (1+m^q)^2\right) L^2T^{2q} \end{aligned} \quad (28)$$

Then, adding $V_{k+m-1} = \frac{1}{2} \|x_c(t_{k+m-1})\|^2$ to both sides of the inequality, we see that:

$$\begin{aligned} V_{k+m} &\leq \frac{1}{2}\left(1 - \frac{1}{\alpha}\right)^2 \|x_c(t_{k+m-1})\|^2 \\ &+ \frac{1}{2}\left(1 - \frac{1}{\alpha^2} + \left(1 - \frac{1}{\alpha}\right)(1+m^q)\right)LT^q \|x_c(t_{k+m-1})\| \\ &+ \frac{1}{8}\left(\left(1 + \frac{1}{\alpha}\right)^2 + \frac{4}{\alpha}(1+m^q) + (1+m^q)^2\right) L^2T^{2q} \\ &= \tilde{a} \|x_c(t_{k+m-1})\|^2 + \tilde{b} \|x_c(t_{k+m-1})\| + \tilde{c} \end{aligned} \quad (29)$$

where $\tilde{a}, \tilde{b}, \tilde{c}$ are strictly greater than 0, and $\tilde{a}h_2^2 + \tilde{b}h_2 + \tilde{c} = \frac{1}{2}h_2^2$. Therefore, by Lemma 4.3, $V_{k+m} < \frac{1}{2}h_2^2 \leq \max\{V_k, \frac{1}{2}h_2^2\}$ for all $\|x_c(t_{k+m-1})\| \leq h_2$.

Since it is known that

$$\begin{aligned} \max\{V_{k+1}, \dots, V_{k+m-1}\} &\leq \max\{V_k, \frac{1}{2}h_1^2\} \\ &\leq \max\{V_k, \frac{1}{2}h_2^2\} \end{aligned} \quad (30)$$

And we have shown that for arbitrary V_{k+m-1} , $V_{k+m} \leq \max\{V_k, \frac{1}{2}h_2^2\}$, it follows that

$$W_{k+m} = \max\{V_{k+1}, \dots, V_{k+m}\} \leq \max\{V_k, \frac{1}{2}h_2^2\}$$

If $W_k > \frac{1}{2}h_2^2$, it decreases as $k \rightarrow \infty$, until $W_k \leq \frac{1}{2}h_2^2$, and is thereafter bounded by $\frac{1}{2}h_2^2$. In terms of $\|\mathbf{x}_c(t_k)\|$, this means that $\|\mathbf{x}_c(t_k)\|$ converges to a neighborhood of size h_2 about the origin; that is, the centroid of the targets remains within h_2 of the center of the camera's FOV. \blacksquare

We have shown that $\|\mathbf{x}_c\|$ converges to an invariant neighborhood of 0, with upper bound defined by h_2 . This bound will tend to be conservative, as we have always assumed a worst-case estimation error for the state of each of the targets. However, it is a useful metric for estimating the performance of the networked camera tracking system given computation and communication delay and asynchronicity.

V. SIMULATION

The above camera tracking system is simulated in Matlab for both the single-target and the two-target asynchronous measurement case. Arbitrary deterministic 2-dimensional trajectories are assigned to the targets. It was assumed that the camera system can observe the location of each object with additive Gaussian white noise.

Given the nonlinear dynamics of the targets and measurement noise, it is desirable to use a short-memory filter to estimate the state x from a given observation. A polynomial predictor (implemented using Matlab `polyfit` function) was used to estimate the state at each control instant. The ten most recent data points were used to find a least-squares second-order polynomial function for x_1 and x_2 over time.

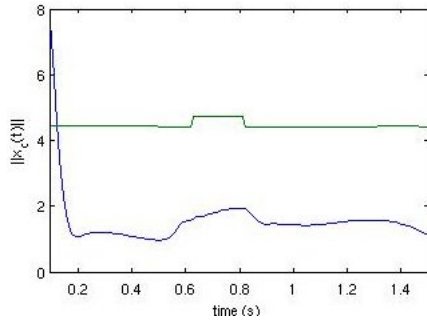


Fig. 3. Distance of target to center of CI's FOV (blue), and theoretical bound (green). The bound is higher when one or both of the targets are occluded.

The simulation was run with $T = 10^{-3}$ sec and m varying between 1 (target not occluded) to 5 (target occluded). A section of the target space was designated “brush area”, with targets becoming occluded whenever they entered this area. As illustrated in fig. 3, the estimates of the size of the neighborhood of the center of the camera's FOV in the previous sections tend to be much higher than the neighborhoods obtained in simulation. This is not surprising, since we have always assumed a worst-case scenario, and calculated bounds on $V(\mathbf{x}_c(t))$ corresponding to maximum possible error at every measurement instant. It may be observed, however, that the size of the neighborhood to which x converges is dependent on the control interval T and on measurement frequency, as expected from our model and calculations.

VI. CONCLUSION

In this paper we have studied the behavior of a camera tracking system in which multiple pan/tilt-enabled cameras are used to track a set of targets in an environment where occlusions can occur. If a target is occluded in a given camera's field of view, the camera can request estimates of the target's position and velocity from cameras which have line of sight with the given target. The states of the different targets are therefore available asynchronously. There is also a delay associated with communications. We have shown that, applying the controller described in (8) to a 2-target system, we can maintain the centroid of the targets within some neighborhood of size h about the center of the camera's field of view. The value of h depends on the control/measurement interval T , and the communication interval mT for obtaining estimates for occluded targets. If a certain performance is required, it can be achieved by adjusting the control and communication intervals. This can be helpful in developing a real-time scheduling control for camera systems, or similar systems in which delay and asynchronicity play a significant

role. In the future, we will consider the effect of stochastic measurement intervals on the performance of the tracking system. The results developed here will be adapted and used to analyze the performance of formation control for groups of underwater robots, which experience extremely long delays and significant asynchronicity in the available measurements.

REFERENCES

- [1] S. Velipasalar, J. Schlessman, C.-Y. Chen, W. Wolf, and J. P. Singh, “SCCS: a scalable clustered camera system for multiple object tracking communicating via message passing interface,” in *Proc. International Conference on Multimedia and Expo*, 2006.
- [2] L. Dugard and E. I. Verriest, *Stability and control of time-delay systems*, ser. Lecture notes in control and information sciences ; 228. London ; New York: Springer, 1998.
- [3] M. S. Mahmoud, *Robust control and filtering for time-delay systems*. New York: Marcel Dekker, 2000.
- [4] J. K. Hale, *Functional differential equations*. New York,: Springer-Verlag, 1971.
- [5] M. Malek-Zavarei and M. Jamshidi, *Time-delay systems : analysis, optimization, and applications*. New York, N.Y., U.S.A.: Elsevier, 1987.
- [6] M. Cao, A. Morse, and B. Anderson, “Agreeing asynchronously in continuous time,” *Proc. 2006 IEEE Conference on Decision and Control*.
- [7] J. N. Tsitsiklis and D. Bertsekas, “Distributed asynchronous routing in data communication networks,” *IEEE Transactions on Automatic Control*, vol. 31, pp. 325–332, 1986.
- [8] A. Balluchi, P. Murrieri, and A. L. Sangiovanni-Vincentelli, “Controller synthesis on non-uniform and uncertain discrete-time domains,” in *HSCC 2005, LNCS 3414*, M. Morari and L. Thiele, Eds. Springer-Verlag, 2005, pp. 118–133.
- [9] J. Grizzle and J.-M. Kang, “Discrete-time control design with positive semi-definite Lyapunov functions,” *Systems and Control Letters*, vol. 40, no. 3, pp. 329–342, 1984.
- [10] T. Hu and Z. Lin, “Absolute stability analysis of discrete-time systems with composite quadratic Lyapunov functions,” *IEEE Transactions on Automatic Control*, vol. 50, no. 6, pp. 781–797, 2005.
- [11] C. Macnab and G. D’Eleuterio, “Discrete-time Lyapunov design for neuroadaptive control of elastic-joint robots,” *International Journal of Robotic Research*, vol. 19, no. 5, pp. 511–525, 2000.
- [12] K. M. Passino, A. N. Michel, and P. J. Antsaklis, “Lyapunov stability of a class of discrete event systems,” *IEEE Transactions on Automatic Control*, vol. 39, no. 2, pp. 269–279, 1994.
- [13] M. S. Branicky, “Multiple Lyapunov functions and other analysis tools for switched and hybrid systems,” *IEEE Trans. Automat. Cont.*, vol. 43, pp. 475–482, 1998.
- [14] Z.-P. Jiang and Y. Wang, “Input-to-state stability for discrete-time nonlinear systems,” *Automatica*, vol. 37, pp. 857–869, 2001.
- [15] E. Sontag, “Further facts about input to state stabilization,” *IEEE Trans. Automatic Control*, vol. 35, no. 4, pp. 435–443, 1990.
- [16] —, “Smooth stabilization implies coprime factorization,” *IEEE Trans. Automatic Control*, vol. 34, no. 4, pp. 473–476, 1989.
- [17] D. Nesić and A. R. Teel, “Input-to-state stability of networked control systems,” *Automatica*, vol. 40, no. 12, pp. 2121–2128, 2004.
- [18] W. P. Dayawansa, B. K. Ghosh, C. Martin, and W. Xiaochang, “A necessary and sufficient condition for the perspective observability problem,” *Systems and Control Letters*, vol. 25, no. 3, pp. 159–66, 1995.
- [19] B. K. Ghosh and E. P. Loucks, “A perspective theory for motion and shape estimation in machine vision,” *SIAM Journal on Control and Optimization*, vol. 33, no. 5, pp. 1530–59, 1995.
- [20] L. Ma, C. Cao, N. Hovakimyan, W. E. Dixon, and C. Woolsey, “Range identification in the presence of unknown motion parameters for perspective vision systems,” in *Proc. 2007 American Control Conference*, New York, 2007, pp. 972–977.
- [21] F. Zhang, K. Szwaykowska, V. Mooney, “Task Scheduling for Control Oriented Requirements for Cyber-Physical Systems,” in *Proc. 2008 Real-Time Sys. Symposium*, Washington, D.C., 2008, pp. 47–56.